



General and Emergency Radiology **Review Article**

## Multimodality imaging of adrenal gland pathologies: A comprehensive pictorial review

Rinald Paloka<sup>1</sup>, Dheeraj Reddy Gopireddy<sup>1</sup>, Mayur Virarkar<sup>1</sup>, Samuel Joseph Galgano<sup>2</sup>, Ajaykumar Morani<sup>3</sup>, Padma Adimula<sup>1</sup>, Anastasia Singareddy<sup>1</sup>, Matthew Montanarella<sup>1</sup>

<sup>1</sup>Department of Radiology, University of Florida Jacksonville, Jacksonville, Florida, <sup>2</sup>Department of Radiology, University of Alabama at Birmingham, Birmingham, <sup>3</sup>Department of Radiology, University of Texas MD Anderson, Houston, Texas, United States.



**\*Corresponding author:**

Rinald Paloka,  
Department of Radiology,  
University of Florida  
Jacksonville, Jacksonville,  
Florida, United States.

[rpaloka2018@health.fau.edu](mailto:rpaloka2018@health.fau.edu)

Received : 08 August 2022  
Accepted : 16 November 2022  
Published : 02 December 2022

DOI  
10.25259/JCIS\_92\_2022

**Quick Response Code:**



### ABSTRACT

The assessment of acute abdominal and pelvic emergencies typically involves a multimodal approach consisting of plain radiographs, ultrasound, computed tomography (CT), and rarely magnetic resonance imaging (MRI). Although MRI is not traditionally employed in acute care settings, there are several instances in which MRI provides superior functional and prognostic information. In this manuscript, we highlight multimodal findings of adrenal gland emergencies: Hemorrhage, infarction, and infection. The purpose of our study is to highlight significant findings in various modalities, including CT, MRI, ultrasound, and PET/CT. Due to the scarcity of published data and limited clinical use, primary ultrasound findings are limited in our multimodal review. In conclusion, we find that synergistic use of CT, MRI, and functional imaging provides an effective tool for evaluation and management of adrenal pathology.

**Keywords:** Multimodality, Adrenal, Emergencies, Computed tomography, Ultrasound, Magnetic resonance imaging, Infection, Neoplasm, Hemorrhage, Infarction

### INTRODUCTION

Clinical signs of adrenal emergencies are non-specific, consisting of abdominal or flank pain, with associated nausea and/or vomiting.<sup>[1]</sup> The presentation with an adrenal crisis is an extremely rare but potentially fatal outcome. Prompt radiographic imaging is necessary to accurately diagnose patients suspected of acute adrenal emergencies. Ultrasonography can be useful in such scenarios in neonates and infants but is less useful in adults. Computed tomography (CT) is the most common imaging modality used for initial evaluation. Although magnetic resonance imaging (MRI) has been used to diagnose incidental or non-emergent pathology, there is limited literature on its use in the field of adrenal emergencies [Table 1].<sup>[2]</sup> The use of a multimodal approach combines the strengths of individual imaging modalities and has a synergistic effect in improving diagnostic yield. This article reviews key radiological features associated with the emergent and non-emergent adrenal pathologies: Hemorrhage, infarction, and infection. We include a comprehensive visual guide for the use of multimodality imaging in diagnosing these conditions and their differentiation from common pathologic mimics.

This is an open-access article distributed under the terms of the Creative Commons Attribution-Non Commercial-Share Alike 4.0 License, which allows others to remix, transform, and build upon the work non-commercially, as long as the author is credited and the new creations are licensed under the identical terms.

©2022 Published by Scientific Scholar on behalf of Journal of Clinical Imaging Science

**Table 1:** Normal appearance of adrenal glands on ultrasound, CT, and MRI.

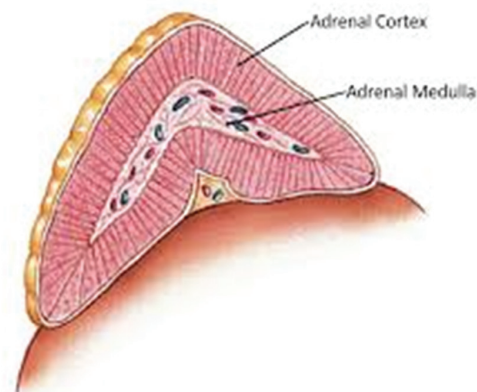
	Ultrasound (US)	CT	MRI
Normal findings	Echogenic “Y-shaped” configuration. Often difficult to identify due to echogenicity of retroperitoneal fat. Predominantly used for neonates/children <sup>[39]</sup>	Bilateral lambdoid structures. Left adrenal typically appears “thickened” relative to right. Contrast enhancement to ~50–60 HU <sup>[21]</sup>	Hyperintensity of surrounding fat. Hypointensity relative to liver on T1- and T2-weighted images <sup>[14,15]</sup>

## ADRENAL ANATOMY

The adrenal (suprarenal) glands are two triangular-shaped glands that are located on top of each kidney and play a significant role in endocrine regulation. Each gland weighs approximately 4–5 g and measures 5 × 2 cm.<sup>[3]</sup> Functionally, they are composed of two units; the inner medulla and the outer cortex [Figure 1]. The glands have a medial and lateral limb and are located in the superior renal fascia within the perirenal space.<sup>[2-5]</sup> Microscopically, the adrenal cortex has three layers: Zona glomerulosa, zona fasciculata, and zona reticularis. These layers produce mineralocorticoids, glucocorticoids, and androgens, respectively.<sup>[3]</sup> The adrenal medulla is responsible for the production of epinephrine and norepinephrine.<sup>[2-6]</sup> Blood supply to the adrenals is derived from inferior phrenic arteries, aorta, and renal arteries through their superior, middle, and inferior adrenal artery branches, respectively [Figure 2].<sup>[7]</sup> These arteries branch further into smaller vessels and eventually supply the adrenal glands with a rich plexus of arterioles and capillary blood.<sup>[7]</sup> This blood flows through a small number of venules in the sinusoids of the corticomedullary junction.<sup>[7,8]</sup> Despite the number of arteries supplying blood, the adrenal gland only has one route of venous drainage through a single central vein.<sup>[8]</sup> Blood pooling in this microvasculature is called adrenal damming.<sup>[7,8]</sup> This anatomy makes the adrenal gland prone to hemorrhage.<sup>[9]</sup>

## EMBRYOLOGY

The cortex and medulla of the adrenal glands have two distinct embryological origins.<sup>[10]</sup> The adrenal cortex is derived from the mesoderm.<sup>[10,11]</sup> A group of mesothelial cells within the urogenital ridge called the adrenal-gonadal primordium gives rise to the primitive fetal adrenal cortex.<sup>[12,13]</sup> At week 6 of fetal development, another group of mesothelial cells surrounds this primitive cortex and forms the permanent cortex.<sup>[4,10,11]</sup> By 8 weeks, this cortical mass detaches from the mesothelium and becomes surrounded by connective tissue.<sup>[4,10]</sup> In contrast, the adrenal medulla is derived from the neuroectoderm.<sup>[10]</sup> At around week 7 of the development, ectodermal cells from the neural crest develop into chromaffin cells, which migrate toward the developed permanent cortex. Gradually, the cortex engulfs these cells and encapsulates the medulla.<sup>[10-12]</sup> Differentiation

**Figure 1:** Adrenal gland medulla and cortex.

of the adrenal cortex into three distinct functional zones is completed by 3 years of age.<sup>[11]</sup>

## ADRENAL EMERGENCIES

### Adrenal hemorrhage

Hemorrhage in the adrenal glands most commonly occurs in the setting of blunt abdominal trauma. Less common causes of adrenal hemorrhage include bleeding diathesis and intratumoral bleeding.<sup>[14]</sup> The prevalence of traumatic and non-traumatic adrenal hemorrhage is between 1.9% and 5.5%.<sup>[15]</sup> Patients with adrenal hemorrhage may experience acute abdominal pain, vomiting, nausea, blood pressure variation, and altered mentation.<sup>[16]</sup> Extensive bilateral adrenal hemorrhage can also cause the development of secondary adrenal insufficiency which ultimately may even lead to death if not discovered promptly.<sup>[17,18]</sup> Evaluation of adrenal hemorrhage through a multimodal approach is critical to patient care in an emergent setting [Figure 3].

Ultrasonography is the modality of choice in infants due to their small body size, relatively large adrenal glands, and due to the lack of ionizing radiation.<sup>[19]</sup> Early-stage hematomas may appear as a solid structure with diffuse or heterogeneous echogenicity. As liquefaction occurs, the mass demonstrates mixed echogenicity with a hypoechoic region, eventually becoming completely anechoic and cyst-like. Calcification of the hematoma walls may be evident as early as 2 weeks

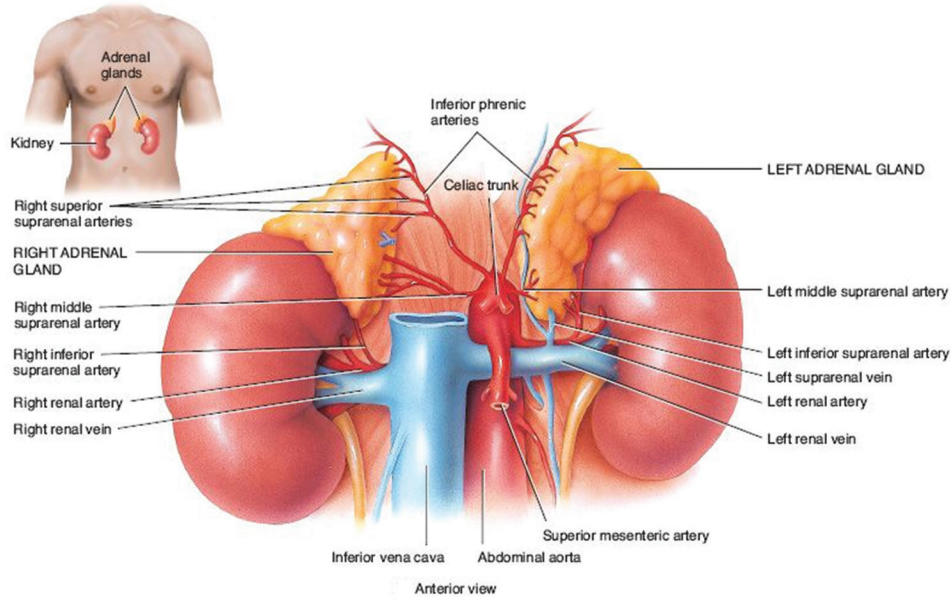


**Figure 2:** Adrenal glands and arterial supply within the retroperitoneum.

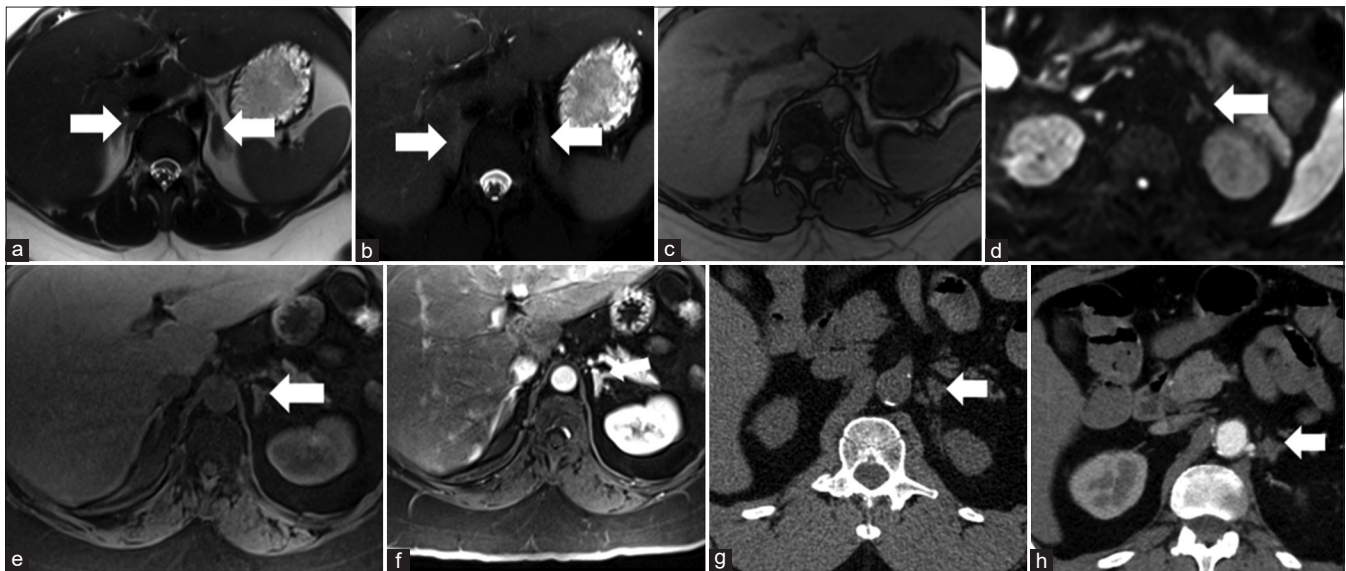


**Figure 3:** A 48-year-old asymptomatic woman with a normal adrenal gland. Normal MRI and computed tomography of adrenal glands. (a) Axial T2 non-fat saturation image. (b) Axial T2 fat saturation image. (c) Axial T1 out-of-phase image. (d) Axial DWI b-500 image. (e and f) Axial pre-T1 and post-contrast T1 image. (g and h) Pre- and post-contrast image of the left adrenal gland (arrow).

after onset, as blood is absorbed [Figure 4].<sup>[19]</sup> Color and power Doppler imaging would aid in evaluating the blood supply of the mass, with hemorrhage typically demonstrating absent flow. Contrast-enhanced ultrasound has been useful in pediatric populations to differentiate between adrenal hemorrhage and masses.<sup>[20]</sup>

CT imaging is currently the imaging of choice for identifying adrenal hemorrhage. Hematomas present as a well-defined nodular mass with a density of 50–80 HU, often associated

with periadrenal fat stranding [Figure 4]. Although the central mass is non-enhancing, enhancement may be preserved in the peripheral architecture presenting a train-track appearance.<sup>[21]</sup> Borders of the adrenal gland may be poorly defined in case of laceration; however, this is a less common cause of hemorrhage.<sup>[22,23]</sup> Chronic hemorrhage eventually presents as an adrenal pseudocyst or adrenal atrophy. On CT, pseudocysts present as non-enhancing masses with central hypodensity and are typically unilocular and peripherally



calcified. Inflammatory reactions due to fat necrosis may result in tracer uptake with hypermetabolism in both acute and chronic adrenal hemorrhages on the F-18 FDG PET study. Determining a neoplastic origin of hemorrhage may be challenging. The absence of central enhancement and calcifications on imaging is characteristics that favor the non-neoplastic etiology.<sup>[24]</sup>

MRI has the added benefit of being able to chronologically grade the hemorrhage.<sup>[14,19,25]</sup> as the breakdown products of hemoglobin dictate appearance and dating.<sup>[14]</sup> This leads to varied appearances on T1- and T2-weighted imaging during evolving periods of bleeding. Hyperacute hemorrhage appears isointense on T1-weighted imaging and hypointense on T2-weighted imaging.<sup>[14,15]</sup> In the acute phase, between 24 and 48 h, as oxyhemoglobin is predominant intracellularly, the hematoma will appear hypointense on T1- and T2-weighted imaging.<sup>[14,15]</sup> Between days 2 and 7, it appears hyperintense on T1-weighted imaging and hypointense on T2-weighted imaging due to the methemoglobin [Figures 5 and 6].<sup>[14,15]</sup> In the subacute phase, between 1 and 2 weeks old, the hematoma will appear hyperintense on both T1- and T2-weighted imaging.<sup>[14,15,26]</sup> After 2 weeks, the hematoma shows a concentric ring of low T1 and T2 signal with a central area of T1 isointense and T2 hyperintensity.<sup>[14]</sup> Chronic stage (>7 weeks) is characterized by the hypointense rim on T1- and T2-weighted images secondary to hemosiderin deposition.

### Trauma

Patients that experience blunt abdominal trauma are at risk for adrenal hemorrhage. About 80% of adrenal hemorrhages have a traumatic etiology.<sup>[27]</sup> Adrenal hemorrhage in the setting of trauma can occur bilaterally but tends to be more common in the right gland.<sup>[15,28]</sup> Located deep within the retroperitoneum, the gland is relatively protected from traumatic injury. The adrenal glands are injured in up to 4% of severe blunt abdominal traumas.<sup>[29]</sup> Patients with trauma and adrenal hemorrhage have higher mortality than those with uninvolved glands.<sup>[30]</sup> Isolated adrenal gland trauma is rare and is typically associated with pulmonary contusions, solid abdominal organ lacerations, axial skeleton fractures, and head injury. Associated findings include posterior pararenal space hemorrhage, IVC compression, psoas muscle hematoma, and thickening of the diaphragmatic crus.<sup>[22,23]</sup>

CT is currently the gold standard in the assessment of trauma patients. MRI has not been routinely used for emergent adrenal gland imaging in the setting of trauma due to its cost and time requirement, but its added benefit includes the ability to use gadolinium when iodinated contrast with CT may be contraindicated. It also provides the ability to use imaging in populations that cannot be exposed to radiation.<sup>[31]</sup>

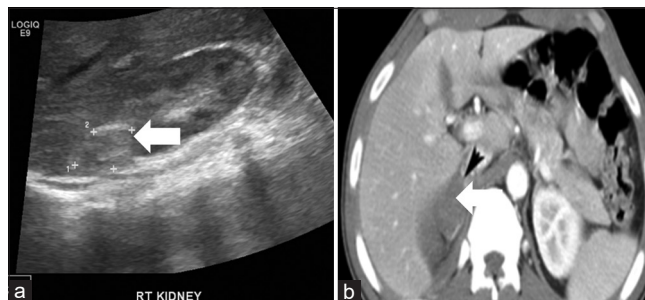


**Figure 4:** A 56-year-old man presented with adrenal hemorrhage and presenting with abdominal pain. (a) Axial ultrasound image demonstrates resolving hematoma characterized by a hyperechoic rim (arrow), likely peripheral calcification, within the right adrenal gland. (b) In contrast-enhanced axial computed tomography image, there is acute hematoma (arrow) with peri adrenal fat stranding.

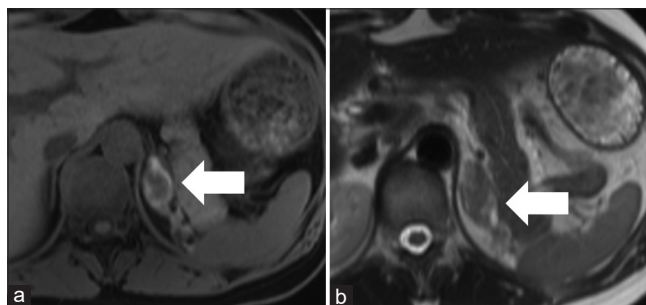


**Figure 5:** A 41-year-old man presented with adrenal hemorrhage and presenting with difficulty breathing and hypotension. (a) T1- and (b) T2-weighted MRI images of adrenal hemorrhage. Hyperintensity on T1-weighted image (a) and hypointensity on T2-weighted image (b) are consistent with early subacute hematoma (arrow).

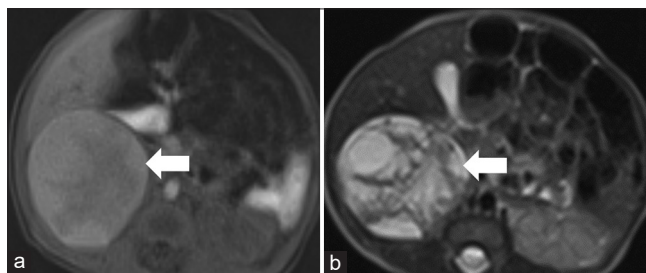


**Figure 6:** A 22-day-old female presented with adrenal hemorrhage and presenting with abdominal pain. Axial (a) pre-contrast T1- and (b) T2-weighted images demonstrated large adrenal hemorrhage (arrow) in a neonate with sepsis. T1- (a) and T2 (b)-weighted hyperintensity is consistent with subacute hemorrhage between 1 and 2 weeks old.

### Stress

Adrenal hemorrhage may be associated with stress secondary to surgery, hypotension, pregnancy, sepsis, or burns. Massive bilateral hemorrhage may be evident in critically ill patients. Risk factors increase due to anticoagulant therapy or bleeding

diathesis. The proposed mechanism involves increased adrenocorticotropic hormone release, resulting in increased adrenal blood flow.<sup>[19,32]</sup> More so, catecholamine-induced vasoconstriction reduces outflow, which results in worsening of the intraglandular hemorrhage.<sup>[19]</sup> On CT, bilateral adrenal hyperenhancement has been suggested to occur in >60% of patients with hypotension. During the arterial phase, there is increased peripheral zone enhancement giving a mosaic appearance [Figure 7]. Complete enhancement may be seen in the venous phase.<sup>[33]</sup> Non-enhancing foci may also be evident, particularly if associated with necrosis or infarction [Figure 8]. Additional findings may include unilateral or bilateral hemorrhage of varying severity.

### Neoplasm

Adrenal intratumoral bleeding is a cause for concern in non-traumatic patients. Primary adrenal tumors and cysts have been reported to be the fourth most common cause of retroperitoneal hemorrhage.<sup>[19]</sup> Acute hemorrhage in an adrenal tumor most commonly occurs with pheochromocytomas, but this type of bleeding can also occur in other primary and metastatic adrenal tumors.<sup>[19,21]</sup> A series of 204 patients with spontaneous adrenal hemorrhage demonstrated that underlying adrenal pathology was not discovered in most of these patients until they exhibited shock-like symptoms or upon autopsy. Adrenal neoplasms were discovered in 20% of these patients.<sup>[34,35]</sup> Although there is limited research on the pathophysiology of adrenal hemorrhage due to neoplasm, possible mechanisms of intratumoral bleeding include vascular fragility, blood vessel invasion, and tumor size outgrowing blood supply.<sup>[34,35]</sup> CT imaging criteria and characterization of adrenal masses in the presence of hemorrhage are highly variable.<sup>[5,36]</sup> Differentiating between tumoral and non-tumoral hemorrhage may be difficult. The presence of intralesional calcifications, enhancement, and hypermetabolic activity on PET may be indicative of an underlying tumor.<sup>[21]</sup> MRI can be useful in detecting the presence of an underlying mass in patients who have exhibited acute or subacute adrenal bleeding. The presence of blood products obscures the details and may result in an overall heterogeneous, hyperdense appearance of the mass.<sup>[35]</sup> However, MRI is overall the most sensitive and specific modality for diagnosing adrenal hemorrhage and is especially useful in determining the age of a hematoma.<sup>[37]</sup>

### Adenoma

Adrenal adenomas are the most common adrenal tumor. It is a benign tumor arising from the cortex, typically found incidentally. Due to its benign and hypovascular nature, massive hemorrhage is extremely rare.<sup>[19]</sup> Adenomas are typically homogenous and <4 cm in diameter. Approximately 70% of tumors are lipid rich, demonstrating hypoattenuation

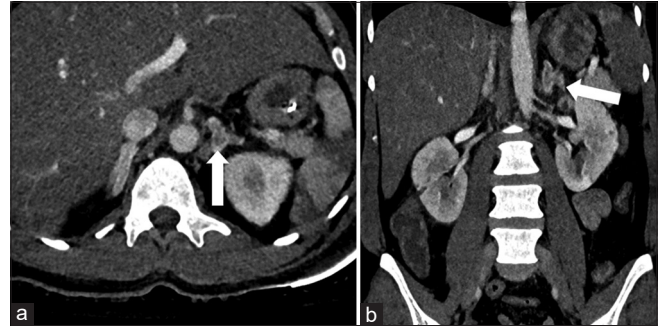


**Figure 7:** A 28-year-old man presented with adrenal hyperenhancement and presenting with hypotension. Axial (a) and coronal (b) arterial phase post-contrast computed tomography (CT) abdomen images of a patient with acute shock demonstrate enhancement of the adrenal gland cortex (arrow) and are consistent with the shock stress state and form part of the CT hypoperfusion complex.

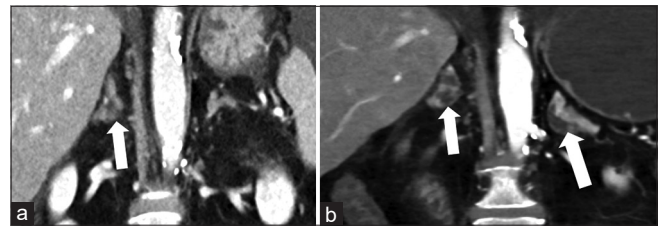


**Figure 8:** A 67-year-old female with adrenal infarcts presented with severe Gram-negative sepsis and tachycardia. (a and b) Coronal contrast-enhanced computed tomography images demonstrate non-enhancing foci in the adrenal glands compatible with adrenal infarctions.

(<10 HU) on non-enhanced CT. CT washout can be used to diagnose higher attenuating masses: An absolute washout of >60% and a relative washout of >40% are generally diagnostic. In patients with relative contraindications to ionizing radiation or CT contrast, chemical shift MRI may be used as an alternative in diagnosing higher attenuating masses. On MRI, lipid-rich adenomas show signal drop on out-of-phase sequences.<sup>[26]</sup> In one study, it was found that a signal intensity drop of 20% correlated with 67% sensitivity for hyperattenuating adenomas (>10 HU) on non-enhanced CT.<sup>[38]</sup> In other words, adenomas appear darker in out-of-phase images due to intravoxel signal cancellation of lipid and water protons. In non-lipid containing masses such as metastasis, there should be no significant signal loss.<sup>[27]</sup> Adenomas may have a variable degree of hypermetabolism on F-18 FDG PET/CT; however, activity is usually less intense than adjacent liver background activity.<sup>[26,39]</sup>

### Myelolipoma

Adrenal myelolipomas are relatively uncommon tumors and are composed of mature fatty tissue and bone marrow. It has been suggested that at least 50% of the mass must have

macroscopic fat for the definitive diagnosis of myelolipoma. The exact prevalence of the tumor is difficult to estimate given the high number of asymptomatic cases and its benign nature.<sup>[40]</sup> Size ranges are typically from 2 cm to 13 cm and symptomatic presentation is typically due to hemorrhage or mass effect.<sup>[26]</sup> Hemorrhage is more common in tumors with a diameter >10 cm with spontaneous rupture being reported in tumors as small as 7 cm.<sup>[41]</sup> Although the literature on pathogenesis is limited, myelolipomas may be more prone to hemorrhage due to intratumoral aneurysms and vascular ectasia. Due to the fatty components, they appear hyperechoic on ultrasound imaging. On CT, the mass shows low attenuation (<-30 HU) due to macroscopic fat with interspersed hyperattenuating bone marrow.<sup>[19,26]</sup> On MRI, areas of fat are hyperintense on T1 images with loss of signal on fat-suppressed sequences [Figure 9]. Adrenal myelolipomas typically demonstrate lower uptake than adjacent liver, although rare cases have been noted in the literature.<sup>[1,42]</sup>

#### Adrenocortical carcinoma (ACC)

ACC is the most common primary malignant adrenal tumor with frequent metastasis to the liver, lung, or bones. These tumors are highly aggressive and may invade local vasculature, resulting in hemorrhage and distant metastasis.<sup>[19]</sup> Poor prognostic factors at presentation include sharp back pain, shock, and retroperitoneal hemorrhage.<sup>[19,26]</sup> On imaging, they are typically large (>6 cm) heterogeneous masses with areas of central hemorrhage or necrosis [Figure 10].<sup>[19,26]</sup> Calcifications and the presence of venous infiltration are characteristic findings. The absolute percentage washout (APW) and relative percent washout (RPW) are <60 and 40%, respectively; however, this finding may also be seen in metastasis.<sup>[1,26]</sup> ACC is typically intensely FDG avid due to elevated mitotic rate. The degree and volume of tracer uptake have been reported to be representative of tumor burden and are a useful tool in identifying primary tumors, recurrence, and metastasis, and determining prognosis.<sup>[1,24]</sup> In one study

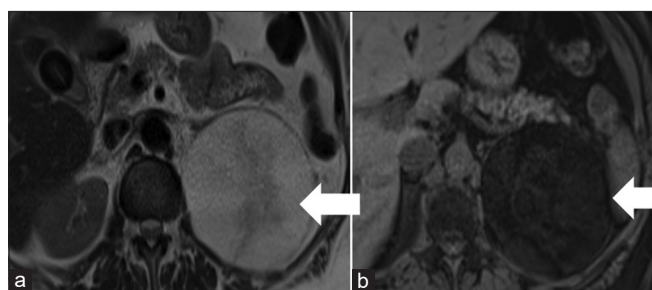


**Figure 9:** A 45-year-old male presented with adrenal myelolipoma and presenting with the left flank pain. (a) Axial non-fat saturating T2-weighted and (b) pre-contrast T1-weighted images demonstrated a large fatty mass (arrow) arising from the superior pole of the left kidney. Biopsy was consistent with adrenal myelolipoma.

of 28 patients, an FDG PET uptake intensity of >10 SUV or uptake volume of >150 mL was associated with 6-month mortality in 54 and 55% of patients, respectively.<sup>[24]</sup>

#### Pheochromocytoma

Pheochromocytomas are adrenal medullary tumors arising from chromaffin cells. They are the most common bilateral primary adrenal gland tumor with an incidence of 10%.<sup>[26,43]</sup> Pheochromocytomas have been reported to be the most common cause of massive hemorrhage from a primary adrenal tumor.<sup>[19]</sup> Clinical presentation is typical of catecholamine excess including refractory hypertension, flushing, headache, and palpitations; however, approximately 10% are clinically silent.<sup>[26]</sup> On CT, they appear as enhancing masses and may even show APW and RPW >60% and 40%, respectively. An absolute washout of >110–120 HU is highly suggestive of pheochromocytoma. Large tumors are heterogeneous, demonstrating central necrosis, hemorrhage, and cystic components. MRI typically demonstrates T1 hypointensity, T2 hyperintensity, and contrast enhancement. Hemorrhage or necrosis may demonstrate altered signal intensity [Figure 11].<sup>[19,26]</sup> Overall, functional imaging alone is limited due to poor specificity. When used with CT or MRI, octreotide and I-123 metaiodobenzylguanidine (MIBG) can aid in whole-body scans and staging. Any focal uptake of I-123 MIBG has been reported to have a sensitivity of approximately 80–90% while uptake of In-111 octreotide has a reported sensitivity of 75–90%. When used complementarily, nearly all pheochromocytomas demonstrate uptake either one or both agents.<sup>[27]</sup> Increased 18F-FDG uptake on PET is typically present and is a useful alternative to tumors that are not MIBG avid.<sup>[26,39]</sup>

#### Neuroblastic tumors

Neuroblastic tumors may arise anywhere along the sympathetic chain; however, the majority of tumors arise in the adrenal medulla. Neuroblastomas represent the most common extracranial pediatric malignancies.<sup>[26,44]</sup> Clinical presentation includes pain, abdominal distension, or neurologic deficits. Initial presentation in neonates includes massive intra-abdominal hemorrhage, resulting in life-threatening abdominal compartment syndrome.<sup>[44]</sup> On plain films, neuroblastic tumors may present as retroperitoneal mass with calcifications in 30% of cases. Ultrasonography may reveal a heterogeneous mass with anechoic areas corresponding to hemorrhage or necrosis. CT is the gold standard in assessing neuroblastic tumors. Large tumors are typically heterogeneous demonstrating calcifications in 80–90% of cases.<sup>[44]</sup> Areas of necrosis or hemorrhage may be noted as areas of low attenuation within the mass. Characteristic features include vascular encasement, midline crossing, and extension into the spinal canal. On MRI,



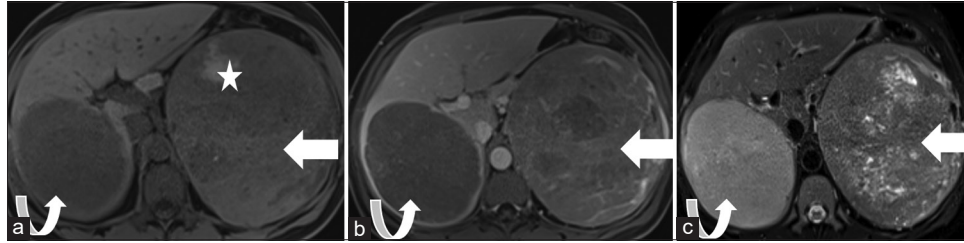


**Figure 10:** A 52-year-old female presented with adrenal carcinoma and presenting with abdominal distension. Axial (a) pre-contrast T1, (b) post-contrast T1, and (c) T2-weighted images show a large heterogeneous mass arising from the left adrenal gland (arrow). Notice the intrinsic T1 signal on the pre-contrast image showing hemorrhage (star). Metastasis is also noted in the posterior segment of the right hepatic lobe (curved arrow). Pathology demonstrated adrenal carcinoma.

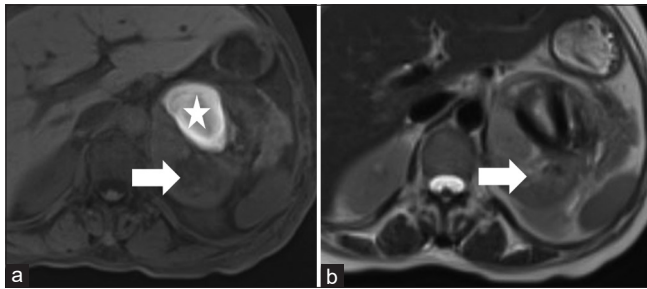


**Figure 11:** A 41-year-old male presented with pheochromocytoma and presenting with uncontrolled hypertension. Axial (a) T1-weighted and (b) T2-weighted MRI images demonstrate a large mass in the left adrenal gland (arrow) with an intrinsic high signal (star) on T1-weighted images secondary to hemorrhage in a pheochromocytoma.

tumors are typically variably enhancing hypointense on T1 and hyperintense on T2.<sup>[44]</sup> Hemorrhages will present as hyperintensities on T1W images. MIBG is typically used for primary tumor identification and whole-body staging. FDG PET may be performed when the tumor is not MIBG avid and technetium-99m MDP can be used for the evaluation of bone disease.<sup>[26,44]</sup>

#### Metastasis

Adrenals are a common site for metastasis, typically arising from primary lung, breast, gastrointestinal, prostate, melanoma, or kidney cancer.<sup>[19,26]</sup> Although hemorrhagic adrenal metastasis is rare, bronchogenic carcinoma has been reported to be the most common cause.<sup>[19]</sup> On CT, the typical presentation includes attenuation of >10 HU with relative and absolute post-contrast washouts <40 and 60%, respectively. Poorly defined contours due to perirenal infiltration may be evident.<sup>[19]</sup> MRI demonstrates contrast enhancement with no signal drop on out-of-phase images, helping differentiate from benign adenomas [Figure 12].<sup>[26]</sup> Increased uptake on FDG PET relative to the adjacent liver may help to differentiate from a benign lesion, but one should be cautious as adrenal adenomas may also be sometimes

hypermetabolic.<sup>[26,39]</sup> In such cases, rapid interval growth is the most helpful feature to differentiate metastasis. It has been reported that up to 90% of adrenal metastasis from lung cancer demonstrate a significant FDG uptake.<sup>[1]</sup>

#### PERIRENAL HEMORRHAGE: A MIMIC OF ADRENAL HEMORRHAGE

When evaluating hemorrhage of the adrenal glands, it is entirely possible that the blood is not actually in the adrenal gland itself but rather in the perirenal space. This hemorrhage may rarely be spontaneous with an unknown etiology, result from trauma, medical procedures involving the kidney, or related to underlying renal neoplasms.<sup>[45-48]</sup> Like adrenal hemorrhage, MRI evaluation of a perirenal hematoma can give insight into the timeline of bleeding and help discover an underlying mass to be the cause on follow-up studies.<sup>[49]</sup> In perirenal hemorrhage, gadolinium contrast should be non-enhancing.<sup>[49]</sup>

#### Adrenal infarction

Although rare, adrenal infarction may be a source of acute abdominal pain. Clinical findings include severe flank pain, guarding, and adrenal insufficiency. Most commonly, infarction occurs bilaterally and is related to the adrenal hemorrhage.<sup>[50]</sup> The central adrenal vein is composed of thick, longitudinal muscle bundles, predisposing it to turbulent flow, and subsequent thrombosis during stress.<sup>[19]</sup> In a prior study, 33 of 78 cases of adrenal hemorrhage demonstrated adrenal vein thrombosis.<sup>[51]</sup> Increased incidence has been reported in hypercoagulable states including factor V Leiden, heparin-induced thrombocytopenia, DIC, trauma, hypothermia, or severe infection.<sup>[50-52]</sup> CT findings may demonstrate diffuse adrenal edema and enlargement. Specific findings include overflowing thrombi from the right adrenal vein to the inferior vena cava. In addition, hyperdensities in the adrenal parenchyma, perirenal fat stranding, and poor cortical enhancement corresponding to necrosis may be seen.<sup>[5]</sup>

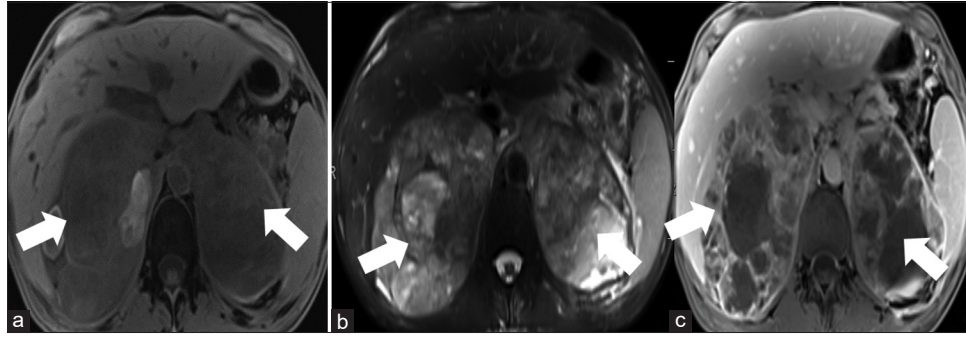


**Figure 12:** A 75-year-old male presented with bilateral adrenal metastases from lung adenocarcinoma and presenting with shortness of breath. (a) Axial T1-weighted, (b) axial T2-weighted, and (c) post-contrast T1-weighted images show bilateral large heterogeneous masses arising from bilateral adrenal glands (arrows) compatible with bilateral adrenal metastasis.

Adrenal infarction associated with pregnancy is a unique scenario, occurring most commonly due to an inherent hypercoagulable state, and may be a cause of severe abdomen or flank pain and emergency room visits.<sup>[50]</sup> Adrenal infarction was identified in 1.3% of abdominal MRIs in pregnant patients presenting with abdominal or flank pain.<sup>[31]</sup> More so, the antiphospholipid syndrome has been reported as a significant risk factor in pregnant patients.<sup>[51,53]</sup> Furthermore, evaluation of abdominal pain in pregnant women poses a challenge due to radiation exposure, altered anatomy, and the physiology of pregnancy.<sup>[31,54]</sup> MRI has routinely been used to diagnose more common causes of abdominal pain in pregnant women such as biliary, urologic, gynecologic, and gastrointestinal disorders.<sup>[55]</sup> MRI can also be useful in effectively characterizing infarction of the adrenals in pregnant patients.<sup>[31,54,56]</sup> Edema of the adrenal glands and retroperitoneum is best seen with T2-weighted fat-saturated MR imaging.<sup>[7,31]</sup> Adrenal infarction may also demonstrate restricted diffusion with signal loss while on diffusion-weighted imaging MRI [Figure 13].<sup>[57,58]</sup>

### Adrenal infection

The adrenal glands can harbor infection from a variety of microorganisms. Pathogens may directly infect the gland, release local or distant toxins, or induce an autoimmune response.<sup>[59,60]</sup> Patients may experience symptoms of Addison's disease if there is significant bilateral damage.<sup>[60,61]</sup> The presentation includes fatigue, anorexia, hypotension, and metabolic derangements. Although immunocompromised patients are at the greatest risk, there are also reports of immunocompetent hosts being affected.<sup>[60]</sup> Endotoxins are believed to upregulate the hypothalamic-pituitary-adrenal axis. Elevated endogenous corticosteroids then alter the normal inflammatory response, predisposing patients to secondary infection.<sup>[60]</sup> In the most severe cases, endotoxins can induce bilateral adrenal hemorrhage, adrenal crisis, and shock termed Waterhouse–Friderichsen syndrome.

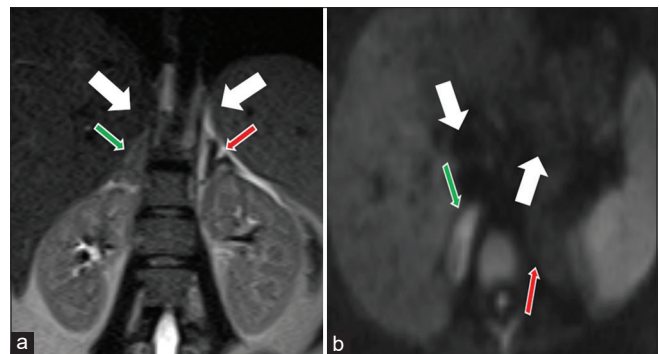


**Figure 13:** A 25-year-old pregnant female presented with the left adrenal infarction and presenting with the left flank pain. (a) Coronal T2-weighted image shows loss of normal signal in the left adrenal gland (red arrow) compared with the normal right adrenal gland (green arrow). (b) Axial DWI image shows loss of normal high DWI signal in the left adrenal gland (red arrow) compared with the normal right adrenal gland (green arrow) and consistent with the left adrenal infarction.

Although *Neisseria meningitidis* is cited as the classic culprit, various other infectious etiologies such as *Streptococcus*, *Haemophilus influenzae*, and *Corynebacterium* have also been reported.<sup>[60]</sup>

### Granulomatous adrenalitis

The adrenal gland is commonly involved in granulomatous infections such as disseminated tuberculosis, histoplasmosis, or blastomycosis. Adrenal tuberculosis remains to be one of the most common causes of Addison's disease in the developing countries. Symptoms typically occur when 90% of tissues are destroyed.<sup>[43]</sup> Disseminated infection typically affects the bilateral adrenal glands due to an equal chance of hematogenous or lymphatic spread. Early CT findings include mass-like enlargement of the adrenals with peripheral enhancement and low central attenuation.<sup>[24]</sup> At the later stage (>1 year), the adrenals may be smaller or normal in



**Table 2:** Summary of key imaging findings in adrenal emergencies.

Entity	Key findings: Ultrasound (US)	Key findings: CT	Key findings: MRI
Adrenal hemorrhage (Acute)	Mass-like with diffuse heterogeneity.	Well-defined nodular mass with an attenuation of 50–80 HU <sup>[26]</sup>	Isointense on T1 and hypointense of T2WI <sup>[14,15]</sup>
Adrenal hemorrhage (Subacute)	Mixed echogenicity with central hypoechoic region	Well-defined nodular mass with an attenuation of 50–80 HU <sup>[26]</sup>	Hyperintensity on T1 and T2WI <sup>[14,15]</sup>
Adrenal hemorrhage (Late)	Peripheral calcification with gradual resolution of blood <sup>[19]</sup>	Peripheral calcification with unenhancing central hypoattenuation (pseudocyst) or atrophy	Peripheral calcification with unenhancing central hypoattenuation (pseudocyst) or atrophy
Adrenal adenoma	Hypovascular, homogenous, and hypoechoic lesion with well-defined borders.	Commonly lipid rich (<10 HU).	Signal dropout on opposed-phase images <sup>[26]</sup>
Adrenal myelolipoma	Hypovascular, homogenous, and hyperechoic with regular margins	Hypoattenuating (<-30 HU) fat components with possible punctate calcifications or hemorrhage <sup>[19]</sup>	Hyperintensity of T1WI with loss of signal of fat suppression
Adrenocortical carcinoma	Hypervascular, small, and homogenous or large and heterogeneous secondary to necrosis and hemorrhage.	Irregularly shaped with central necrosis and hemorrhage. Variable enhancement with possible calcification <sup>[7]</sup>	Heterogeneous mass with hyperintensity on T2WI.
Pheochromocytoma	Hypervascular, heterogeneous with possible solid and cystic components	Large heterogeneous mass with necrosis and cystic changes	Hypointensity on T1 and hyperintensity on T2WI with contrast enhancement <sup>[19]</sup>
Neuroblastic tumors	Internally vascular, heterogeneous mass with possible areas of necrosis <sup>[42]</sup>	Heterogeneous mass with calcifications. Hypoattenuating areas of necrosis.	Heterogeneous, with hypointensity of T1 and hyperintensity of T2WI. May cross midline <sup>[13]</sup>
Adrenal metastasis	Hypervascular, typically bilateral and heterogeneous with variable size and margins.	Avidly enhancing mass with poorly defined contours. Periadrenal infiltration may be evident <sup>[19]</sup>	Contrast enhancement with no sign drop on out-of-phase sequence. Hypointensity on T1 and hyperintensity on T2WI <sup>[26,39]</sup>
Adrenal infarction	US: --	Diffuse edema and periadrenal enlargement. Parenchymal hyperdensities, fat stranding, and poor cortical enhancement due to necrosis <sup>[5]</sup>	Adrenal and retroperitoneal edema on T2W fat-saturated image. Restricted diffusion with signal loss on DWI. <sup>[55,56]</sup> Thrombi may be present <sup>[49]</sup>
Granulomatous adrenalitis	Bilateral adrenal enlargement. Heterogeneous appearance	Mass-like enlargement with peripheral enhancement and low central attenuation <sup>[24,41]</sup>	MRI: --
Adrenal abscess	Well-defined cystic mass.	Enhancing fibrous capsule with surrounding inflammation. Hypoattenuation centrally	Hypointensity of T1 and hyperintensity on T2WI <sup>[7,62]</sup>

US: Ultrasound, CT: Computerized tomography, MRI: Magnetic resonance imaging, T1WI: T1-weighted image, T2WI: T2-weighted image, ACTH: Adrenocorticotrophic hormone, HU: Hounsfield unit

size due to fibrosis and calcifications within the lesions.<sup>[24,43]</sup> Additional late findings may include bilateral soft-tissue masses, cystic changes, or calcifications.<sup>[26]</sup> On FDG PET, tuberculosis may mimic malignancy due to increased tracer uptake secondary to granuloma formation.<sup>[24]</sup>

### Adrenal abscess

At times, particularly with disseminated infections, microorganisms in the adrenals lead to abscess formation. Patients with adrenal abscess typically present with long-

standing fevers, rigors, anorexia, and asthenia.<sup>[62,63]</sup> Commonly implicated organisms include *Streptococcus pneumoniae* and *Nocardia*. The classic presentation of abscesses on CT includes low central attenuation, a well-defined enhancing fibrous capsule, and surrounding inflammatory changes. On MRI, adrenal abscesses typically present as T2W-hyperintense and T1W-hypointense cystic lesion with wall enhancement [Figure 14]. MRI has the additional benefit of better characterizing internal contents and identifying periadrenal edema, which would present as a bright signal on T2W images.<sup>[7,64]</sup>

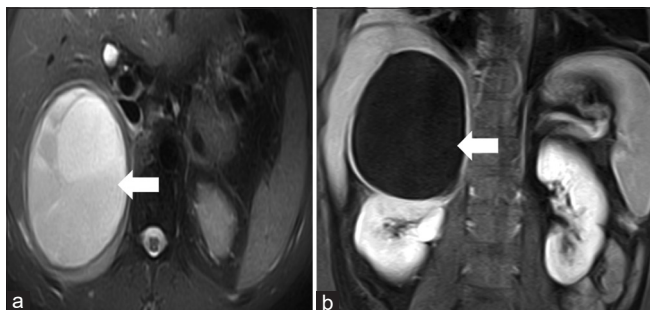


**Figure 14:** A 58-year-old male presented with a right adrenal abscess and presenting with abdominal pain and fever. (a) Axial fat saturation T2-weighted and (b) coronal post-contrast T1 weighted image show a large cystic mass arising from the right adrenal gland (arrow) with wall enhancement compatible with an abscess. Notice there is no nodularity in the wall.

Some adrenal tumors such as myelolipoma have been shown to develop superimposed hemorrhage and abscess formation and require urgent surgical intervention.<sup>[65]</sup> Complex adrenal abscesses may be commonly misdiagnosed as pseudocysts or necrotic adrenal tumors. Characteristics that favor abscess over pseudocyst include round shape, homogenous density, diameter <4 cm, and absence of calcifications. The presence of rapid mass growth and liquefaction has also been described as a useful criterion in differentiating from the malignancy.<sup>[64,66]</sup>

### CYSTIC ADRENAL NEOPLASM: A MIMIC OF ADRENAL INFECTION

Cystic adrenal neoplasms are not the common adrenal pathologies and only consist of a small percentage of adrenal cystic lesions.<sup>[67]</sup> Cysts in the adrenal gland can be separated into four categories: Pseudocysts, epithelial cysts, endothelial cysts, and parasitic cysts.<sup>[67-70]</sup> Endothelial cysts can be further divided into angiomatous and lymphangiomatous cysts and epithelial cysts subdivided into glandular and embryonal cysts.<sup>[67-69]</sup> Cysts of these categories could be detected with adrenal neoplasms. However, these differ from the neoplasms that may exhibit their areas of cystic degeneration.<sup>[68]</sup> Various imaging modalities have proven useful in characterizing cystic lesions of the adrenal glands.<sup>[13,68]</sup> Primary neoplasms that are associated with cysts in the adrenals are classified by the type of primary tumor: Pheochromocytoma, adrenal cortical carcinoma, and adrenal cortical adenoma.<sup>[68]</sup> In these lesions, especially the pheochromocytomas, missing a diagnosis may lead to emergent health consequences. MRI has been the modality of choice for diagnosing pheochromocytomas in patients with clinical signs of the lesion.<sup>[71]</sup> In the largest published case series of cystic adrenal neoplasms, hemorrhage was a major component in a majority of cystic pheochromocytomas and adrenal cortical adenomas.<sup>[68]</sup> Calcifications were present in cystic adrenal carcinomas and

not in pheochromocytomas.<sup>[68]</sup> Pheochromocytomas typically demonstrated bright T2 signal and rapid enhancement with the administration of contrast.<sup>[13,72]</sup> Adrenal carcinomas can exhibit heterogeneous T1W and T2W signals due to necrosis and hemorrhage.<sup>[13]</sup>

### CONCLUSION

This pictorial review presents how a multimodality imaging is useful in assessing adrenal emergencies, including hemorrhage, infarction, and infection [Table 2]. Although CT is currently the gold standard in the assessment of adrenal emergencies, MRI and functional imaging techniques are helpful in difficult or atypical case presentations. MRI modality provides promising results due to recent improvements in soft-tissue contrast, imaging times, and the lack of ionizing radiation. Functional imaging modalities such as F-18 FDG PET and I-123 MIBG aid in the differentiation of disease etiology, whole-body assessment, and prognosis in select cases. Synergistic use of CT, MRI, and functional imaging is an effective tool for accurate evaluation and management of adrenal emergencies.

### Declaration of patient consent

Patients' consent not required as patients' identity is not disclosed or compromised.

### Financial support and sponsorship

Nil.

### Conflicts of interest

There are no conflicts of interest.

### REFERENCES

1. Dong A, Cui Y, Wang Y, Zuo C, Bai Y. (18)F-FDG PET/CT of adrenal lesions. *AJR Am J Roentgenol* 2014;203:245-52.
2. Hussain HK, Korobkin M. MR imaging of the adrenal glands. *Magn Reson Imaging Clin N Am* 2004;12:515-44, vii.
3. Megha R, Wehrle CJ, Kashyap S, Leslie SW. Anatomy, abdomen and pelvis, adrenal glands (suprarenal glands). In *StatPearls*. Treasure Island: StatPearls; 2020.
4. Mitty HA. Embryology, anatomy, and anomalies of the adrenal gland. *Semin Roentgenol* 1988;23:271-9.
5. Peppercorn PD, Reznick RH. State-of-the-art CT and MRI of the adrenal gland. *Eur Radiol* 1997;7:822-36.
6. Mitchell DG, Nascimento AB, Alam F, Grasel RP, Holland G, O'Hara BJ. Normal adrenal gland: *In vivo* observations, and high-resolution *in vitro* chemical shift MR imaging-histologic correlation. *Acad Radiol* 2002;9:430-6.
7. Udare A, Agarwal M, Siegelman E, Schieda N. CT and MR imaging of acute adrenal disorders. *Abdom Radiol (NY)* 2021;46:290-302.

8. Bassett JR, West SH. Vascularization of the adrenal cortex: Its possible involvement in the regulation of steroid hormone release. *Microsc Res Tech* 1997;36:546-57.
9. Mehmood KT, Sharman T. Adrenal hemorrhage. In: *StatPearls*. Treasure Island: StatPearls; 2020.
10. Barwick TD, Malhotra A, Webb JA, Savage MO, Reznek RH. Embryology of the adrenal glands and its relevance to diagnostic imaging. *Clin Radiol* 2005;60(9):953-9.
11. Moore KL, Persaud TV, Torchia MG. *The Developing Human: Clinically Oriented Embryology*. 10<sup>th</sup> ed. Philadelphia, PA: Elsevier; 2016. p. 524.
12. Willenberg HS, Bornstein SR. Adrenal cortex. Development, anatomy, physiology. In: Feingold KR, Anawalt B, Boyce A, Chrousos G, de Herder WW, Dhatariya K, *et al*, editors. *Endotext*: South Dartmouth (MA): MDText. Com, Inc.; 2000.
13. Lockhart ME, Smith JK, Kenney PJ. Imaging of adrenal masses. *Eur J Radiol* 2002;41:95-112.
14. Hammond NA, Lostumbo A, Adam SZ, Remer EM, Nikolaidis P, Yaghami V, *et al*. Imaging of adrenal and renal hemorrhage. *Abdom Imaging* 2015;40:2747-60.
15. Wang F, Liu J, Zhang R, Bai Y, Li C, Li B, Liu H, *et al*. CT and MRI of adrenal gland pathologies. *Quant Imaging Med Surg* 2018;8:853-75.
16. Simon DR, Palese MA. Clinical update on the management of adrenal hemorrhage. *Curr Urol Rep* 2009;10:78-83.
17. Xarli VP, Steele AA, Davis PJ, Buescher ES, Rios CN, Garcia-Bunuel R. Adrenal hemorrhage in the adult. *Medicine (Baltimore)* 1978;57:211-21.
18. Sinelnikov AO, Abujudeh HH, Chan D, Novelline RA. CT manifestations of adrenal trauma: experience with 73 cases. *Emerg Radiol* 2007;13:313-8.
19. Kawashima A, Sandler CM, Ernst RD, Takahashi N, Roubidoux MA, Goldman SM, *et al*. Imaging of nontraumatic hemorrhage of the adrenal gland. *Radiographics* 1999;19:949-63.
20. Back SJ, Acharya PT, Bellah RD, Cohen HL, Darge K, Deganello A, *et al*. Contrast-enhanced ultrasound of the kidneys and adrenals in children. *Pediatr Radiol* 2021;51:2198-213.
21. Jordan E, Poder L, Courtier J, Sai V, Jung A, Coakley FV. Imaging of nontraumatic adrenal hemorrhage. *AJR Am J Roentgenol* 2012;199:91-8.
22. Burks DW, Mirvis SE, Shanmuganathan K. Acute adrenal injury after blunt abdominal trauma: CT findings. *AJR Am J Roentgenol* 1992;158:503-7.
23. Blake MA, Cronin CG, Boland GW. Adrenal imaging. *AJR Am J Roentgenol* 2010;194:1450-60.
24. Leboulleux S, Dromain C, Bonniaud G, Aupérin A, Caillou B, Lumbroso J, *et al*. Diagnostic and prognostic value of 18-fluorodeoxyglucose positron emission tomography in adrenocortical carcinoma: A prospective comparison with computed tomography. *J Clin Endocrinol Metab* 2006;91:920-5.
25. Rubin JI, Gomori JM, Grossman RI, Gefter WB, Kressel HY. High-field MR imaging of extracranial hematomas. *AJR Am J Roentgenol* 1987;148:813-7.
26. Bhargava P, Sangster G, Haque K, Garrett J, Donato M, D'Agostino M. A multimodality review of adrenal tumors. *Curr Probl Diagn Radiol* 2019;48:605-15.
27. Mayo-Smith WW, Boland GW, Noto RB, Lee MJ. State-of-the-art adrenal imaging. *Radiographics* 2001;21:995-1012.
28. Song JH, Mayo-Smith WW. Current status of imaging for adrenal gland tumors. *Surg Oncol Clin N Am* 2014;23:847-61.
29. Chernyak V, Patlas MN, Menias CO, Soto JA, Kielar AZ, Rozenblit AM, *et al*. Traumatic and non-traumatic adrenal emergencies. *Emerg Radiol* 2015;22:697-704.
30. Rana AI, Kenney PJ, Lockhart ME, McGwin Jr, Morgan DE, Windham ST 3<sup>rd</sup>, *et al*. Adrenal gland hematomas in trauma patients. *Radiology* 2004;230:669-75.
31. Glomski SA, Guenette JP, Landman W, Tatli S. Acute nonhemorrhagic adrenal infarction in pregnancy: 10-Year MRI incidence and patient outcomes at a single institution. *AJR Am J Roentgenol* 2018;210:785-91.
32. Hasenmajer V, Bonaventura I, Minnetti M, Sada V, Sbardella E, Isidori AM. Non-canonical effects of ACTH: Insights into adrenal insufficiency. *Front Endocrinol (Lausanne)* 2021;12:701263.
33. Di Serafino M, Viscardi D, Iacobellis F, Giugliano L, Barbuto L, Oliva G, *et al*. Computed tomography imaging of septic shock. Beyond the cause: The "CT hypoperfusion complex". A pictorial essay. *Insights Imaging* 2021;12:70.
34. Vella A, Nippoldt TB, Morris JC 3<sup>rd</sup>. Adrenal hemorrhage: A 25-year experience at the mayo clinic. *Mayo Clin Proc* 2001;76:161-8.
35. Marti JL, Millet J, Sosa JA, Roman SA, Carling T, Udelsman R. Spontaneous adrenal hemorrhage with associated masses: Etiology and management in 6 cases and a review of 133 reported cases. *World J Surg* 2012;36:75-82.
36. Sussman SK, Rosshirt W. Perinephric hemorrhage secondary to adrenal myelolipoma. Case report. *Clin Imaging* 1991;15:299-301.
37. Elsayes KM, Mukundan G, Narra VR, Lewis JS Jr, Shirkhoda A, Farooki A, *et al*. Adrenal masses: Mr imaging features with pathologic correlation. *Radiographics* 2004;24:S73-86.
38. Haider MA, Ghai S, Jhaveri K, Lockwood G. Chemical shift MR imaging of hyperattenuating (>10 HU) adrenal masses: Does it still have a role? *Radiology* 2004;231:711-6.
39. Metser U, Miller E, Lerman H, Lievshitz G, Avital S, Even-Sapir E. 18F-FDG PET/CT in the evaluation of adrenal masses. *J Nucl Med* 2006;47:32-7.
40. Decmann Á, Perge P, Tóth M, Igaz P. Adrenal myelolipoma: A comprehensive review. *Endocrine* 2018;59:7-15.
41. Kenney PJ, Wagner BJ, Rao P, Heffess CS. Myelolipoma: CT and pathologic features. *Radiology* 1998;208:87-95.
42. Jeon HJ, Lee SY. A case of adrenal myelolipoma a patient with breast cancer. *Acta Endocrinol (Buchar)* 2017;13:90-5.
43. Guo YK, Yang ZG, Li Y, Ma ES, Deng YP, Min PQ, *et al*. Addison's disease due to adrenal tuberculosis: Contrast-enhanced CT features and clinical duration correlation. *Eur J Radiol* 2007;62:126-31.
44. Lonergan GJ, Schwab CM, Suarez ES, Carlson CL. Neuroblastoma, ganglioneuroblastoma, and ganglioneuroma: Radiologic-pathologic correlation. *Radiographics* 2002;22:911-34.
45. Azmat R, Siddiqui AB, Khan MT, Sunder S, Kashif W. Bleeding



- complications post ultrasound guided renal biopsy-A single centre experience from Pakistan. *Ann Med Surg (Lond)* 2017;21:85-8.
46. Shoorbridge JJ, Corcoran NM, Martin KA, Koukounaras J, Royce PL, Bultitude MF. Contemporary management of renal trauma. *Rev Urol* 2011;13:65-72.
  47. Zagoria RJ, Dyer RB, Assimos DG, Scharling ES, Quinn SF. Spontaneous perinephric hemorrhage: Imaging and management. *J Urol* 1991;145:468-71.
  48. Bosniak MA. Spontaneous subcapsular and perirenal hematomas. *Radiology* 1989;172:601-2.
  49. Glockner JF, Lee CU. Magnetic resonance imaging of perirenal pathology. *Can Assoc Radiol J* 2016;67:149-57.
  50. Chasseloup F, Bourcigaux N, Christin-Maitre S. Unilateral nonhaemorrhagic adrenal infarction as a cause of abdominal pain during pregnancy. *Gynecol Endocrinol* 2019;35:941-4.
  51. Fox B. Venous infarction of the adrenal glands. *J Pathol* 1976;119:65-89.
  52. Rao RH. Bilateral massive adrenal hemorrhage. *Med Clin North Am* 1995;79:107-29.
  53. Espinosa G, Santos E, Cervera R, Piette JC, de la Red G, Gil V, *et al.* Adrenal involvement in the antiphospholipid syndrome: Clinical and immunologic characteristics of 86 patients. *Medicine (Baltimore)* 2003;82:106-18.
  54. Guenette JP, Tatli S. Nonhemorrhagic adrenal infarction with magnetic resonance imaging features during pregnancy. *Obstet Gynecol* 2015;126:775-8.
  55. Baheti AD, Nicola R, Bennett GL, Bordia R, Moshiri M, Katz DS, *et al.* Magnetic resonance imaging of abdominal and pelvic pain in the pregnant patient. *Magn Reson Imaging Clin N Am* 2016;24:403-17.
  56. Reichman O, Keinan A, Weiss Y, Applbaum Y, Samueloff A. Non-hemorrhagic adrenal infarct in pregnancy-a rare clinical condition diagnosed by non-contrast magnetic resonance image. *Eur J Obstet Gynecol Reprod Biol* 2016;198:173-4.
  57. Moliere S, Gaudineau A, Koch A, Leroi T, Roedlich MN, Veillon F. Usefulness of diffusion-weighted imaging for diagnosis of adrenal ischemia during pregnancy: A preliminary report. *Emerg Radiol* 2017;24:705-8.
  58. Sormunen-Harju H, Sarvas K, Matikainen N, Sarvilinna N, Laitinen EK. Adrenal infarction in a healthy pregnant woman. *Obstet Med* 2016;9:90-2.
  59. Arlt W. Adrenal insufficiency. *Clin Med (Lond)* 2008;8:211-5.
  60. Paolo WF Jr., Nosanchuk JD. Adrenal infections. *Int J Infect Dis* 2006;10:343-53.
  61. Huebener KH, Treugut H. Adrenal cortex dysfunction: CT findings. *Radiology* 1984;150:195-9.
  62. Urrutia A, Santesmases J, Benítez RM, Areal J. Adrenal gland abscess due to *Streptococcus pneumoniae*. *J Infect* 2010;60:88-9.
  63. Tachezy M, Simon P, Ilchmann C, Vashist YK, Izbicki JR, Gawad KA. Abscess of adrenal gland caused by disseminated subacute *Nocardia farcinica* pneumonia. A case report and mini-review of the literature. *BMC Infect Dis* 2009;9:194.
  64. Stankard M, Gopireddy D, Lall C. Role of MRI in the diagnosis of large right adrenal abscess. *Cureus* 2020;12:e10986.
  65. Kumar S, Jayant K, Prasad S, Agrawal S, Parma KM, Roat R, *et al.* Rare adrenal gland emergencies: A case series of giant myelolipoma presenting with massive hemorrhage and abscess. *Nephrourol Mon* 2015;7:e22671.
  66. Midiri M, Finazzo M, Bartolotta TV, Maria MD. Nocardial adrenal abscess: CT and MR findings. *Eur Radiol* 1998;8:466-8.
  67. Rozenblit A, Morehouse HT, Amis ES Jr. Cystic adrenal lesions: CT features. *Radiology* 1996;201:541-8.
  68. Erickson LA, Lloyd RV, Hartman R, Thompson G. Cystic adrenal neoplasms. *Cancer* 2004;101:1537-44.
  69. Abeshouse GA, Goldstein RB, Abeshouse BS. Adrenal cysts; Review of the literature and report of three cases. *J Urol* 1959;81:711-9.
  70. Sebastiano C, Zhao X, Deng FM, Das K. Cystic lesions of the adrenal gland: Our experience over the last 20 years. *Hum Pathol* 2013;44:1797-803.
  71. Andreoni C, Krebs RK, Bruna PC, Goldman SM, Kater CE, Alves MT, *et al.* Cystic pheochromocytoma is a distinctive subgroup with special clinical, imaging and histological features that might mislead the diagnosis. *BJU Int* 2008;101:345-50.
  72. Kier R, McCarthy S. MR characterization of adrenal masses: Field strength and pulse sequence considerations. *Radiology* 1989;171:671-4.

**How to cite this article:** Paloka R, Gopireddy DR, Virarkar M, Galgano SJ, Morani A, Adimula P, *et al.* Multimodality imaging of adrenal gland pathologies: A comprehensive pictorial review. *J Clin Imaging Sci* 2022;12:62.